Report No. HA-39

Centre for Radio Science

DETAILED ANALYSIS OF ANOMALOUS TERRESTRIAL MICROWAVE PROPAGATION DATA AND ASSESSMENT OF ALTERNATIVE EXPERIMENTAL TECHNIQUES

Final Report

DSS Contract No.
03SU.36001-2-1480

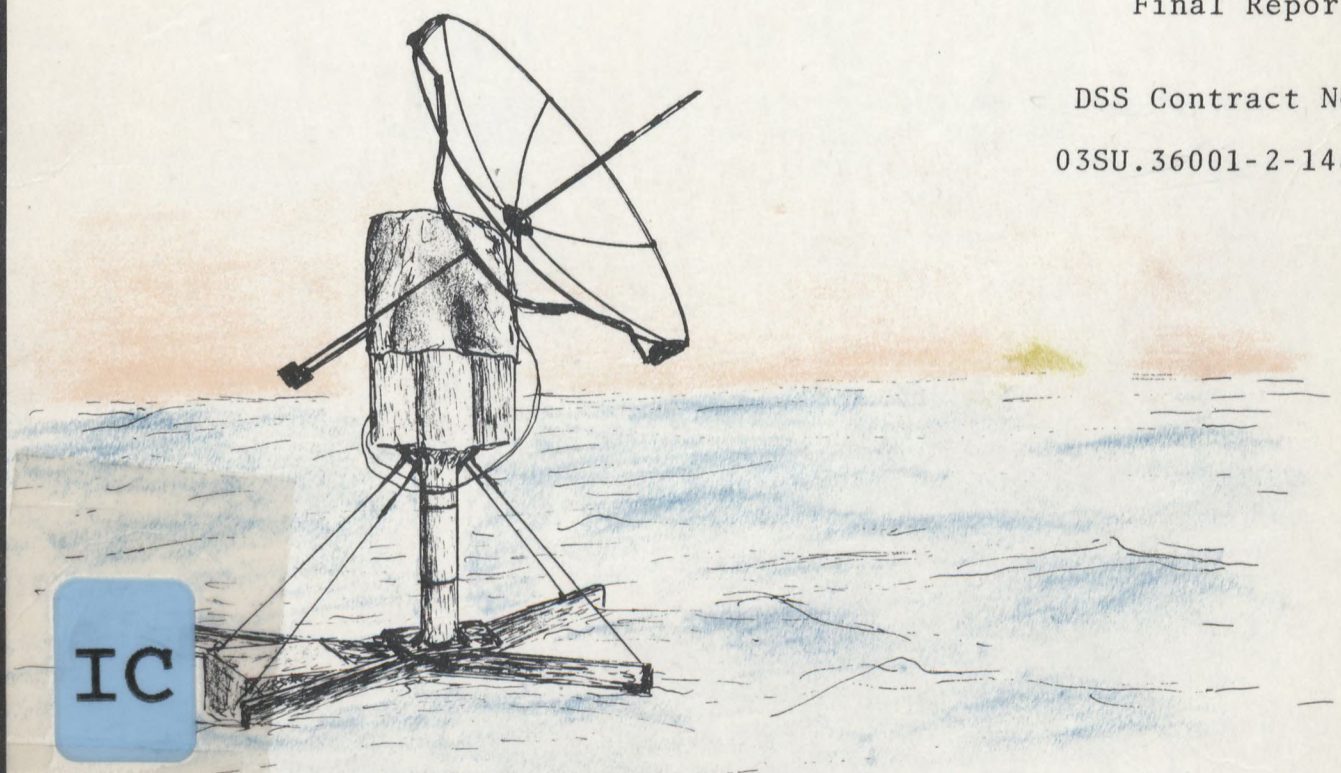

THE UNIVERSITY OF WESTERN ONTARIO
LONDON CANADA N6A 3K7

July, 1983

DETAILED ANALYSIS OF ANOMALOUS TERRESTRIAL MICROWAVE PROPAGATION DATA AND ASSESSMENT OF ALTERNATIVE EXPERIMENTAL TECHNIQUES

A Final Report under
Department of Supplies and Services
Contract No. 03SU.36001-2-1480

Submitted to

Communications Research Centre
Department of Communications, Canada

by

Centre for Radio Science
University of Western Ontario
London, Canada

Principal Investigator: A.R. Webster
Research Associate: W.I. Lam

Report prepared by: W.I. Lam (Part I)
A.R. Webster (Part II)

ABSTRACT

This report consists of two parts. In Part I, the results from two X-band microwave propagation experiments conducted across the Bay of Fundy are presented. The results include statistics on various signal characteristics of ray amplitudes, ray path angle-of-arrival and the relative delay time between rays. Also included are distributions of the received signal fade depth and enhancement. The results substantiate the finding that severe fading across the bay occurs as a result of the combined effects of atmospheric layers and the sea reflection.

Part II of the report deals with some practical aspects of using a wide-aperture antenna array in microwave propagation studies. Such an array is envisaged as a convenient way of measuring the amplitudes and angles-of-arrival of the received ray(s) under various atmospheric conditions. The tests presented in the report indicate that the development of such a wide-aperture system is feasible.

TABLE OF CONTENTS

Part I

STATISTICAL RESULTS ON MICROWAVE PROPAGATION CONDITIONS ACROSS THE BAY OF FUNDY

I.1 INTRODUCTION

During the periods from September to November 1980, and from August to September 1981, two microwave propagation experiments were performed on separate line-of-sight paths across the Bay of Fundy. In the first experiment, the 80.03 km long propagation path was between Otter Lake, NB, and Aylesford, NS, while in the second experiment the 80.38 km path was between Otter Lake, NB, and Nictaux South, NS.

The equipment used in both experiments was a microwave diagnostic system which provided sweep-frequency (9.5 to 10.5 GHz) measurements of received signal amplitude and relative phase on two vertically spaced antennas. The signal characteristics that may be derived from the sweep-frequency data are the amplitudes, angles-of-arrival, and the relative delay times of the ray(s) observed at the receiving antennas. In addition to the diagnostic system, a Northern Telecom RD-3 digital radio was operated concurrently in the 1981 experiment and it provided information pertaining to the performance of such digital systems under various propagation conditions.

Details of the experimental arrangements, as well as results and conclusions drawn from the preliminary analysis of the recorded data, were presented in previous reports [1], [2]. This report contains results obtained through an in-depth analysis of the experimental data. The results presented include statistics on various ray path characteristics of amplitudes, angles-of-arrival, and relative delay times. In addition, distributions of fade depth and signal enhancement are included.

I.2 GENERAL CONSIDERATIONS

I.2.1 BACKGROUND

In order to provide for an independent reading of this report, the main features of the propagation paths and the major results described in previous reports are included.

The path profiles, in flattened earth form, are shown in Figs. I.2.1(a) and (b). Also shown in the figures are the ray paths drawn for a normal atmosphere with dN/dh = -40 NU/km (corresponding to a 4/3-earth model). In both cases, a direct ray and a sea reflected ray are possible with the ray path angles-of-arrival (AOA) as shown. Furthermore, it is noted that the Otter Lake - Nictaux South path in the 1981 experiment was chosen with better terrain blockage to the reflected ray.

Under normal conditions, the amplitude and delay time

of the reflected ray relative to the direct ray was estimated as -19 dB and 2.5 ns for the Otter Lake - Aylesford path, and -30 dB and 4.5 ns for the Otter Lake - Nictaux South path. These values were predicted by using a ray tracing technique and assuming a constant N-gradient of -40 NU/km. Diffraction losses due to terrain blockages, as well as divergence losses due to reflection from a curved surface, are also accounted for.

The results of the experiments presented in previous reports indicate that propagation under quiet conditions are consistent with an atmospheric model of constant refractivity gradient. However, severe fading appears to have been caused by the presence of atmospheric layers which have important influences on the properties of both the direct and reflected rays [2]-[5].

I.2.2 DATA ANALYSIS

Based on experience gained from the preliminary analysis of the experimental data, changes were made to the data analysis routines previously used. This resulted in improvements in the accuracy of various ray path parameters obtained from the sweep-frequency data, as revealed by extensive tests performed on the analysis routines using simulated data records.

The results presented in this report are derived from two data bases. The first data base contains data from ten days in the 1980 experiment. The data selection was based

on a careful inspection of the continuous analog records such that the amount of fading is well represented. As for the second data base, it includes all available data collected in the thirty-five days in the 1981 experiment.

In order to illustrate the observed fading characteristics, each data base was further divided into two categories for analysis, namely "non-fading" and "fading" data. The fading data base was selected such that it includes all data from the hours in which fades exceeding 10 dB were recorded for more than 1 % of the time. The remaining data were then included in the non-fading data.

I.3 STATISTICS ON RAY CHARACTERISTICS

I.3.1 RAY AMPLITUDE STATISTICS

The amplitude statistics of the two strongest received rays are presented in this section. During non-fading periods, the main and second rays are the direct and the reflected rays respectively. Such is not the case during periods of fading, as the reflected ray occasionally exceeds the direct ray in amplitude to dominate as the main ray.

The distributions of ray amplitudes for the two experiments are shown in Figs. I.3.1 and Figs. I.3.2. The measured median amplitudes of the reflected rays during

quiet periods are -13 dB (1980) and -21 dB (1981). These values are large compared with predicted values of -19 dB and -30 dB respectively (see section I.2.1). The discrepancies are attributed to uncertainties in terrain elevations and the assumed tree heights.

Several interesting observations are noted in the results of both experiments:

(a) the large spread in ray amplitudes for the fading data;

(b) the general decrease in the amplitude of the direct ray (due to defocussing) during fading; and,

(c) the increase in the amplitude of the reflected ray (due to increased clearance above the terrain blockages) during fading.

The observations are consistent with the model that severe fading was caused by the presence of atmospheric layers at heights below the antennas [2].

The same amplitude distributions, plotted using Normal Probability Coordinates, are shown in Figs. I.3.3 and I.3.4. The theoretical distributions [6] of the resultant of a Constant vector and a Rayleigh-distributed vector are also plotted for comparison. The power of the Rayleigh vector being -14 dB (Fig. I.3.3(a)) and -10 dB (Fig. I.3.4(a)) relative to the Constant vector. The agreement between the main ray amplitude distributions for the non-fading data with the theoretical "Constant plus Rayleigh" distributions are well demonstrated.

During periods of fading, the large reduction in the main ray amplitude is seen to be accompanied by a relatively modest increase in the reflected ray amplitude. This suggests that fading activities across the bay are mainly caused by the defocussing of the main ray, presumably by atmospheric layers. Finally, it is worth noting that the amplitude distribution of the second ray for the 1980 non-fading data closely approximates that of a log-normal distribution.

I.3.2 MAIN RAY ANGLE-OF-ARRIVAL DISTRIBUTION

As presented in the report on the 1981 experiment [2], some unusual variations in the main ray AOA were previously inferred. In an effort to identify the cause, it was found that the spurious variations resulted from the presence of very short delay rays [7] (relative delay times of the order of fractions of a nanosecond). Subsequently, an alternative approach for extracting the main ray AOA was incorporated. Careful computer simulations verified that the new approach produces reliable AOA results which are relatively insensitive to the presence of short delay rays.

As an illustration, the main ray AOA observed at Nictaux South (1981 experiment) for five consecutive days are shown in Fig. I.3.5. Although spurious results are still observed during certain periods of severe fading (e.g. 20:00-23:00 ADT on August 12, 02:00-03:00 ADT on August 13, and 06:00-08:00 ADT on August 15), most of the

time the AOA results are quite reliable. Two observations on these results are of particular interest:

(a) During quiet periods when atmospheric layers are not evident (e.g. 04:00-15:00 ADT on August 12, 03:00-23:00 ADT on August 14, and all day on August 16), the main ray AOA shows only mild and slow variations.

(b) The main ray AOA is elevated during periods of fading (e.g. 04:00-15:00 ADT on August 13, and 03:00-12:00 ADT on August 15). Once again, the observation is consistent with the explanation that heavy fading across the Bay of Fundy was caused mainly by atmospheric layers occurring at heights below the antennas.

Distribution of the main ray AOA during quiet periods were computed for both experiments and the results are shown in Figs. I.3.6 and I.3.7. In these figures, the ordinate scales were adjusted such that the median AOA values correspond to the values predicted for $dN/dh = -40$ NU/km.

For the 1980 experiment, the 99.8 % range in main ray AOA is 0.32 deg. The corresponding 99.8 % range for the N-gradient is $-102 < dN/dh < 40$ NU/km, which is equivalent to a range in the Effective Earth-radius Factor of $2.9 < K < 0.8$.

For the 1981 experiment, the 99.8 % range in AOA is

0.47 deg. A 99.8 % range in N-gradient of $-161 < dN/dh < 40$ NU/km is observed, equivalent to a range of $-40 < K < 0.8$. The slightly larger range is partly attributed to the fact that this second experiment was performed during the fading season.

It should be pointed out that the experimentally observed 99.8 % ranges in N-gradient are rather small compared with values given in a refractivity atlas [8] for two nearby locations, namely, Portland, Me., and Sable Island, NS. To account for the discrepancies, it is first noted that the values in the refractivity atlas are given for the first 100 m in the atmosphere. The antenna heights in the experiments, however, dictate that the path followed by the direct ray lies within the height range from 100 to 400 m above mean sea level. Although large N-gradients are not unreasonable at heights close to the surface of the bay, it seems less likely that extreme gradients are maintained over the full height range and large horizontal distances in consideration.

I.3.3 DELAY TIME STATISTICS

Distributions of the delay time of the second ray relative to the main ray were computed for both experiments and the results are shown in Figs. I.3.8 and I.3.9. The measured median delay times of the reflected ray for the non-fading data are 2.3 ns (1980) and 4.7 ns (1981). These values are in excellent agreement with the values of 2.5 ns

and 4.5 ns respectively, both predicted by using ray tracing and assuming a constant N-gradient of -40 NU/km.

The delay time distributions for the fading data illustrate the significant increase in the delay time of the reflected ray which accompany fading activities. Values of greater than 5 ns (1980) and 13 ns (1981) were observed during periods of severe fading (compared with values of 2.5 ns (1980) and 4.5 ns (1981) during quiet periods). Such observations again support the explanation that atmospheric layers occurring at heights below the antennas are the main cause of heavy fading across the bay.

The above results have important implications regarding the operation of wideband digital radio systems. These systems are known to be vulnerable to in-band distortion caused by multipath fading. The problems thus associated with long delay rays are at least two-fold. First, consider the simple case of two received rays. The probability of an in-band null occurring on any fixed radio channel increases directly with the delay time [7]. The bit-error-rate (BER) observed on such systems therefore are expected to increase with the delay time value. The second problem is related to frequency diversity protection schemes which are usually employed in digital radio systems as a means of improving system availability. In particular, the effectiveness of frequency diversity protection is severely reduced when long delay subsidiary rays are present [7].

In the 1981 experiment, a digital radio system with a 40 MHz RF bandwidth was used. The results indicate that when two rays with comparable amplitudes are received, the BER observed on such a radio system will be unacceptably high if the relative delay time between the two rays exceed about 8 ns.

I.4 THE STATISTICS OF SIGNAL FADING

Let V be the normalized amplitude of the received signal, and L be the specified signal level. The probability distributions of fade depth, $P(V \leq L)$, and that of signal enhancement, $P(V \geq L)$, are generated by dividing the total number of data points of level $V \leq L$ (and $V \geq L$) by the total sample size. These distributions were computed for both experiments using the signal level at the base frequency (9.5 GHz) of each sweep record. The reference 0 dB level in all cases are the median signal level for the respective experiments.

I.4.1 FADE DEPTH DISTRIBUTIONS

The fade depth distributions for the non-fading data, fading data, and the combined data are shown in Figs. I.4.1(a) and (b) for the 1980 and 1981 experiments. The empirical relationships shown were obtained by a regression technique applied to the results for fade depths

exceeding 15 dB. Also plotted for comparison purposes are the predicted distributions for the worst fading month based on the CCIR formula [9], applied to the respective propagation paths.

For the 1980 experiment, a $P(V \leq L) \propto L^{2.1}$ relationship is observed, while a $P(V \leq L) \propto L^{1.6}$ relationship holds for the 1981 experiment. The more severe fading in the 1981 experiment, despite the better terrain blockage to the sea reflection, is particularly interesting. This observation is attributed to the fact that the second experiment was performed in August during which a higher frequency of occurrence of atmospheric layers is expected. The result well demonstrates the importance of layers as a major cause of severe fading in this geographical area.

In comparing the CCIR predictions with the experimental results, the reader is reminded that the 1980 experiment was not performed during the worst fading month. As for the 1981 results, it is noted that the CCIR prediction is too optimistic by a factor of more than 3 at the 40 dB level.

I.4.2 STATISTICS ON SIGNAL ENHANCEMENT

In general, emphasis is usually placed on signal fading and consequently less is known about the statistics of signal enhancement. The distributions of signal enhancement above the median level are shown in Figs. I.4.2(a) and (b). One of the few sets of published

statistics on signal enhancement are also shown for comparison. These statistics are reported by Stephansen and Mogensen [10] for an over-land microwave link operated at 14 GHz. The much higher probability of occurrence of signal enhancement in the 1981 experiment is noted.

I.5 CONCLUSIONS AND DISCUSSION

Statistics on various received signal characteristics observed on two oversea paths across the Bay of Fundy have been presented. The results are consistent with findings which are given in previous reports.

The main ray AOA statistics for quiet periods suggest that extreme gradients in refractivity are usually not maintained over a large height range and over large horizontal distances.

During periods of fading, the statistical results well support the findings given in the 1981 report [2] that heavy fading activities across the Bay of Fundy are results of the combined effects of atmospheric layers and the sea reflection. When these layers are present at heights below the antennas, the effects are:

(a) defocussing of the direct ray;

(b) increasing the clearance of the reflected ray above the blocking terrain and hence an increased ray amplitude;

(c) elevating the AOA of both the direct and reflected ray relative to the normal values; and,

(d) substantially increasing the value of the relative delay time of the reflected ray.

For a more detailed discussion of the properties of the sea reflection observed across the bay, the reader is referred to Lam [7].

It seems beyond doubt that wideband digital radio systems, such as the one used in the 1981 experiment, will not provide reliable services when strong subsidiary rays with long delay times (exceeding approximately 8 ns) are received. The situation is worse because such long delay rays also significantly reduce the effectiveness of frequency diversity protection, especially when 1xN protection schemes are used.

A few comments concerning the microwave diagnostic system should also be made. The system is quite adequate for identifying the characteristics of received ray amplitudes, relative delay times, and the main ray AOA. However, there are two main limitations of the system. First, subsidiary rays with very short delay times (say, fractions of a nanosecond) are not resolved by the diagnostic system. As revealed by the experimental results, such short dealy rays, in fact, occur more frequently than was expected.

The second limitation is related to the analysis of the sweep-frequency records gathered using the system.

Although it is comparatively easy to extract the main ray AOA from the raw data, such is not the case for the AOA of subsidiary rays. To extract the latter parameter, a time consuming process of pattern synthesis has to be employed. This effectively prevents a full scale study of AOA variations of subsidiary rays -- a parameter which is of great importance in the study of the mechanisms of multipath propagation. Alternative schemes suitable for performing such measurements should be investigated.

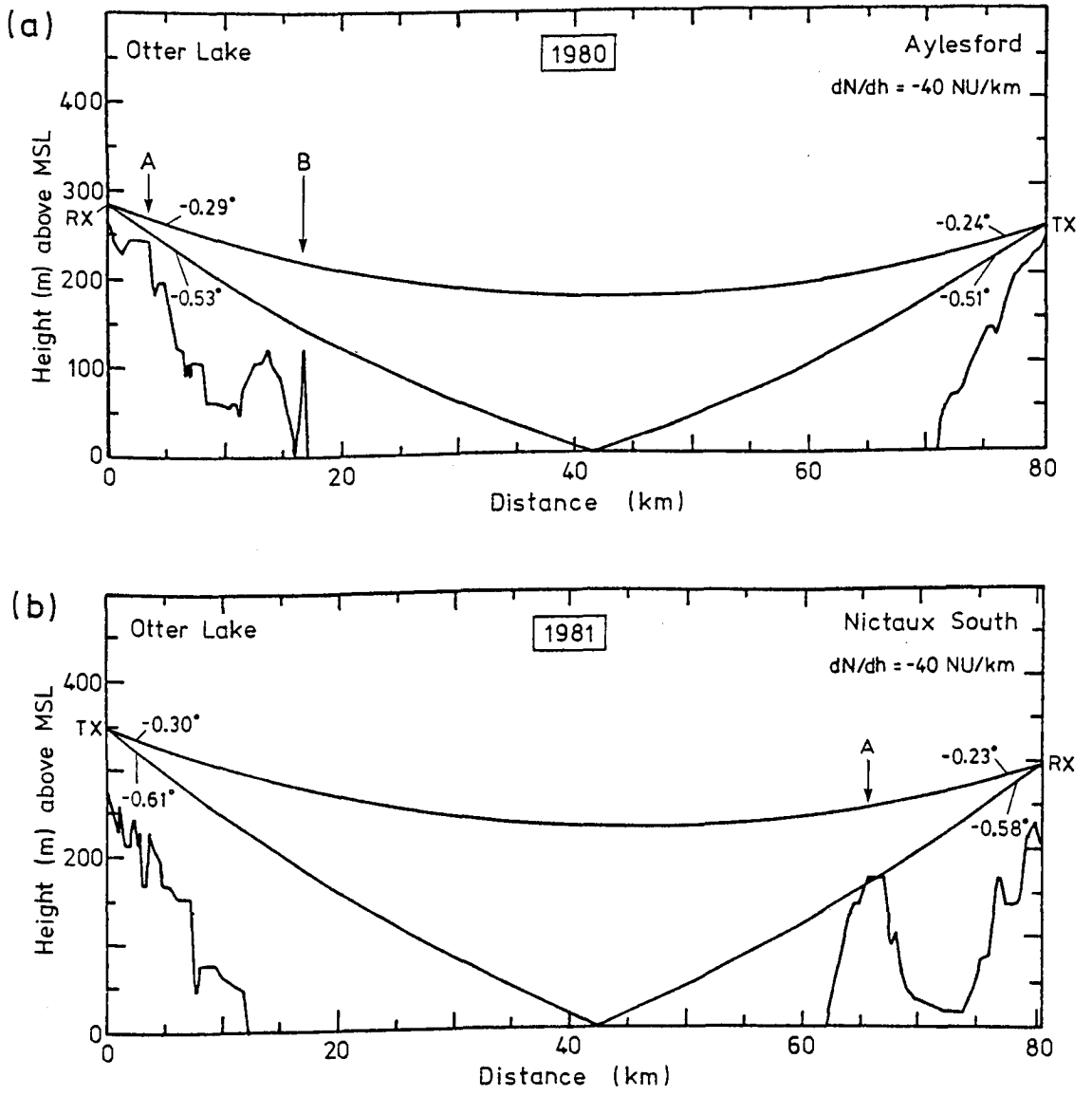

Fig. I.2.1 Profiles of the propagation paths in flattened-earth representation. The ray paths corresponding to 4/3-earth are shown.

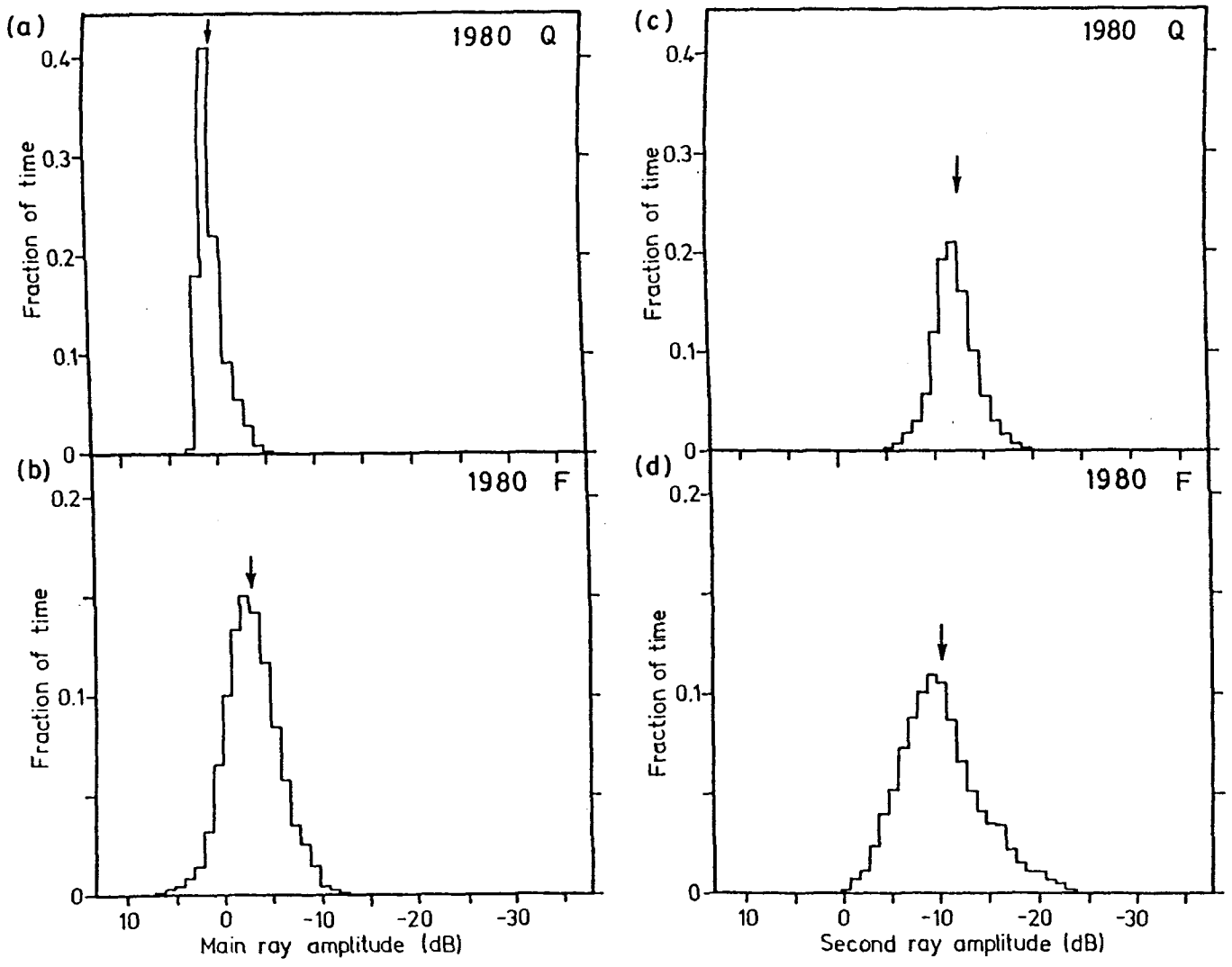

Fig. I.3.1 Distributions of the main and second ray amplitudes during quiet (Q) and fading (F) periods in the 1980 experiment. The arrows mark the median values.

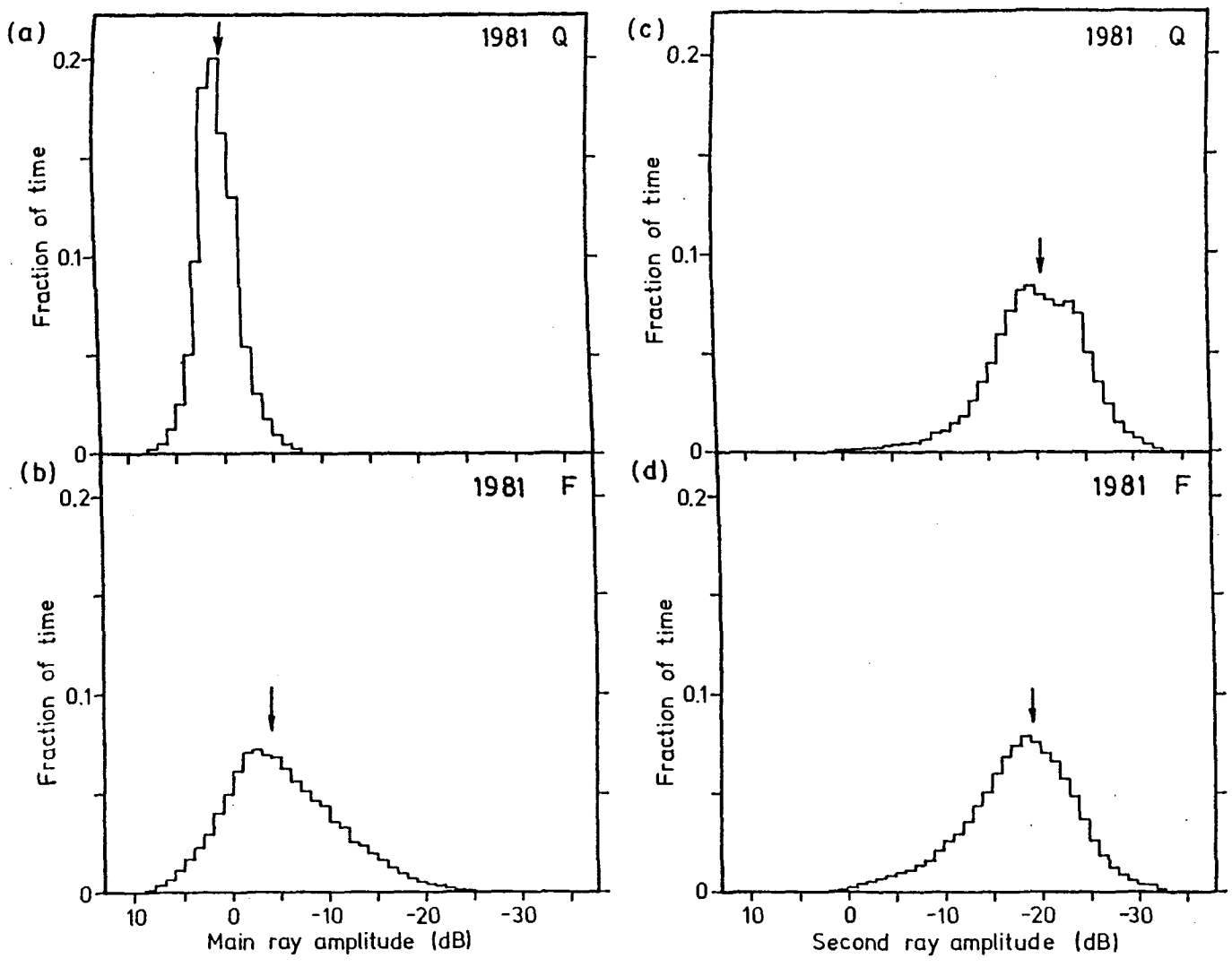

Fig. I.3.2 Distributions of the main and second ray amplitudes during quiet (Q) and fading (F) periods in the 1981 experiment. The arrows mark the median values.

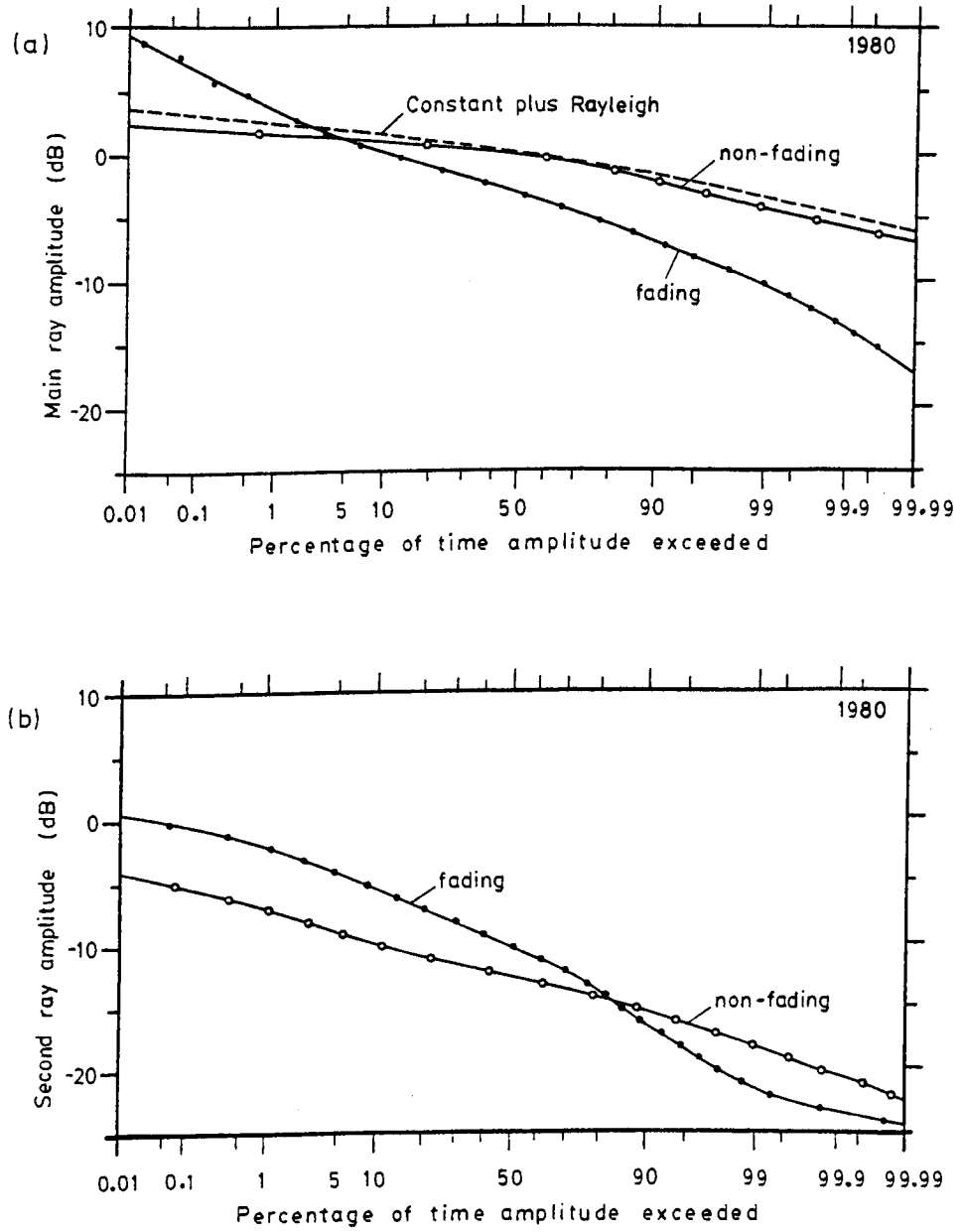

Fig. I.3.3 Distributions of (a) main ray amplitude and (b) second ray amplitude for the 1980 experiment, plotted using Normal Probability Coordinates.

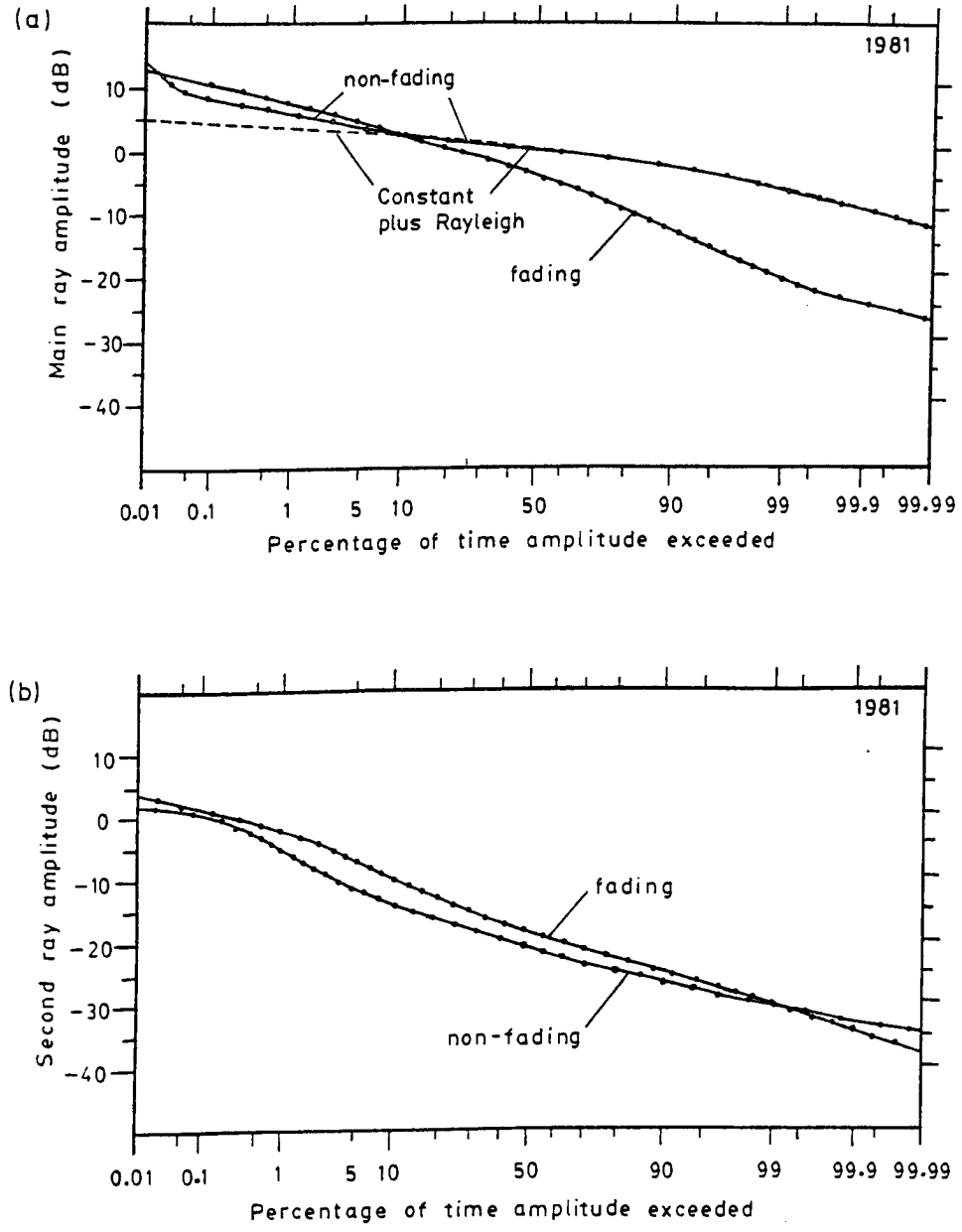

Fig. I.3.4 Distributions of (a) main ray amplitude and (b) second ray amplitude for the 1981 experiment, plotted using Normal Probability Coordinates.

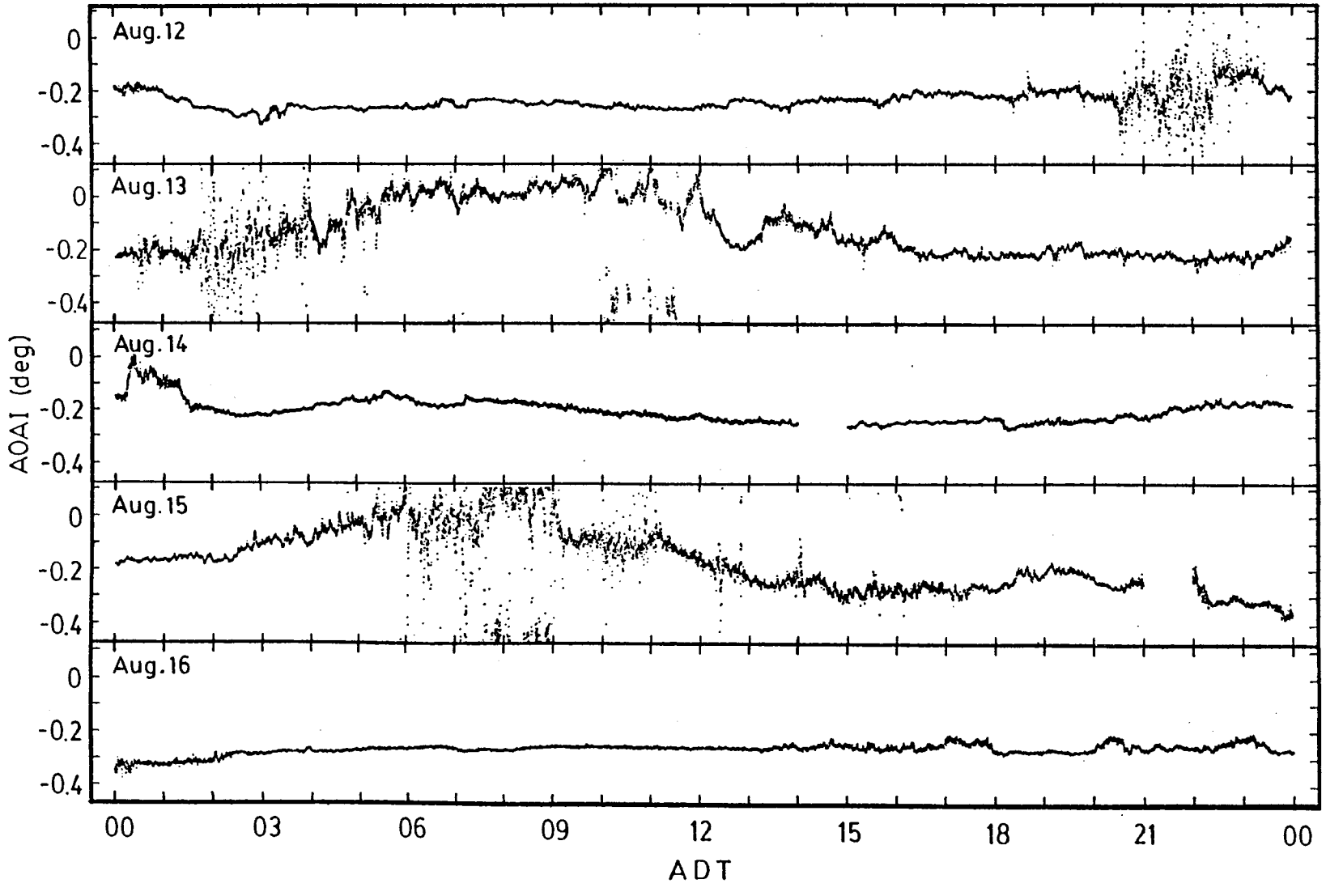

Fig. I.3.5 Main ray angle-of-arrival observed at Nictaux South on five consecutive days during the 1981 experiment.

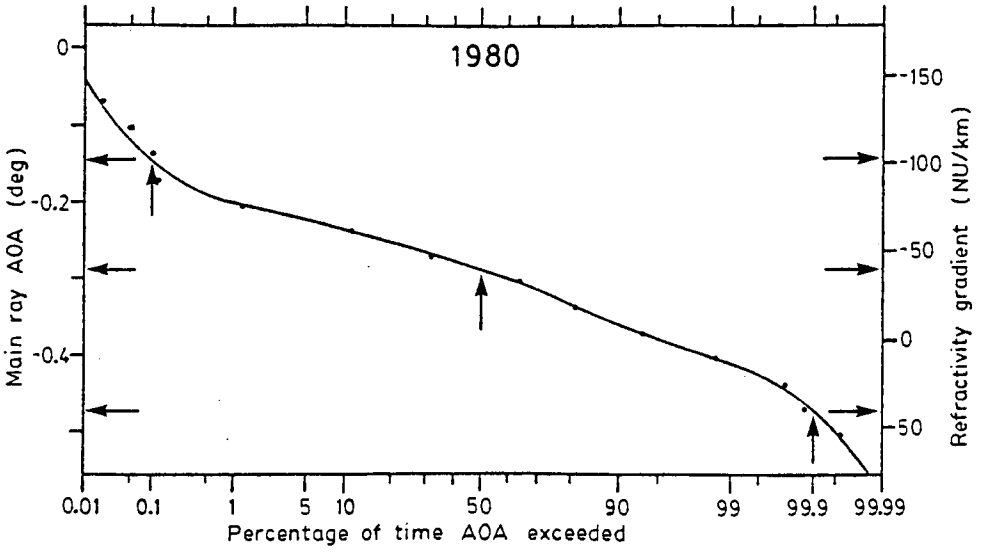

Fig. I.3.6 Distribution of the main ray angle-of-arrival during quiet periods in the 1980 experiment. The arrows mark the 0.1%, 50% and 99.9% values.

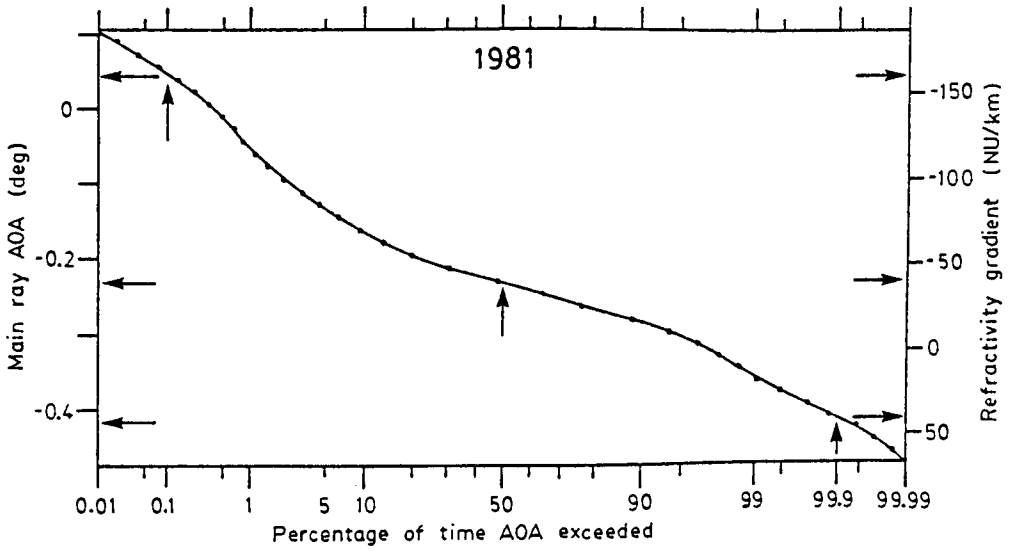

Fig. I.3.7 Distribution of the main ray angle-of-arrival during quiet periods in the 1981 experiment. The arrows mark the 0.1%, 50% and 99.9% values.

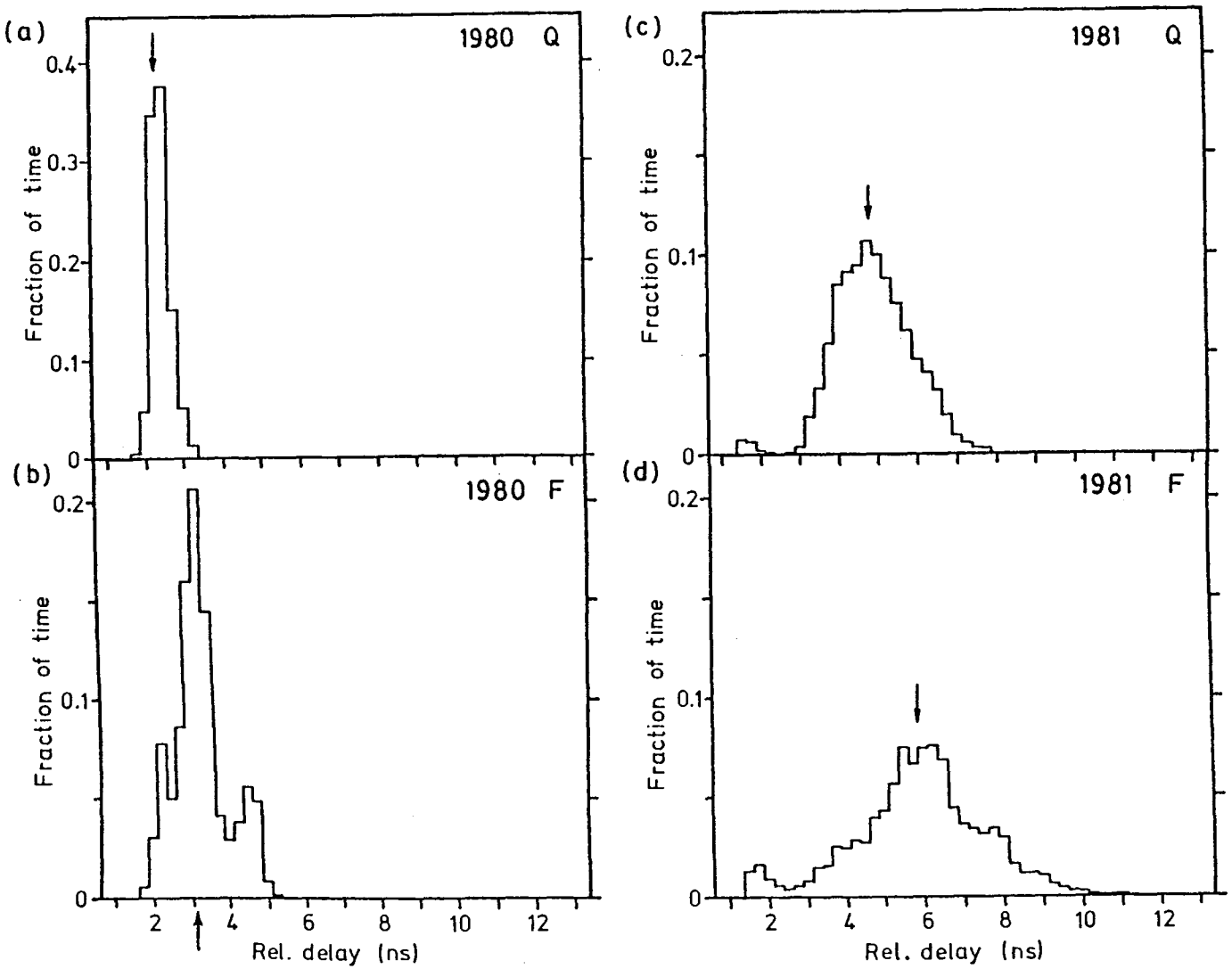

Fig. I.3.8 Distributions of the delay time of the second ray relative to the main ray during quiet (Q) and fading (F) periods in the 1980 ((a) and (b)) and 1981 ((c) and (d)) experiments. The arrows mark the median values.

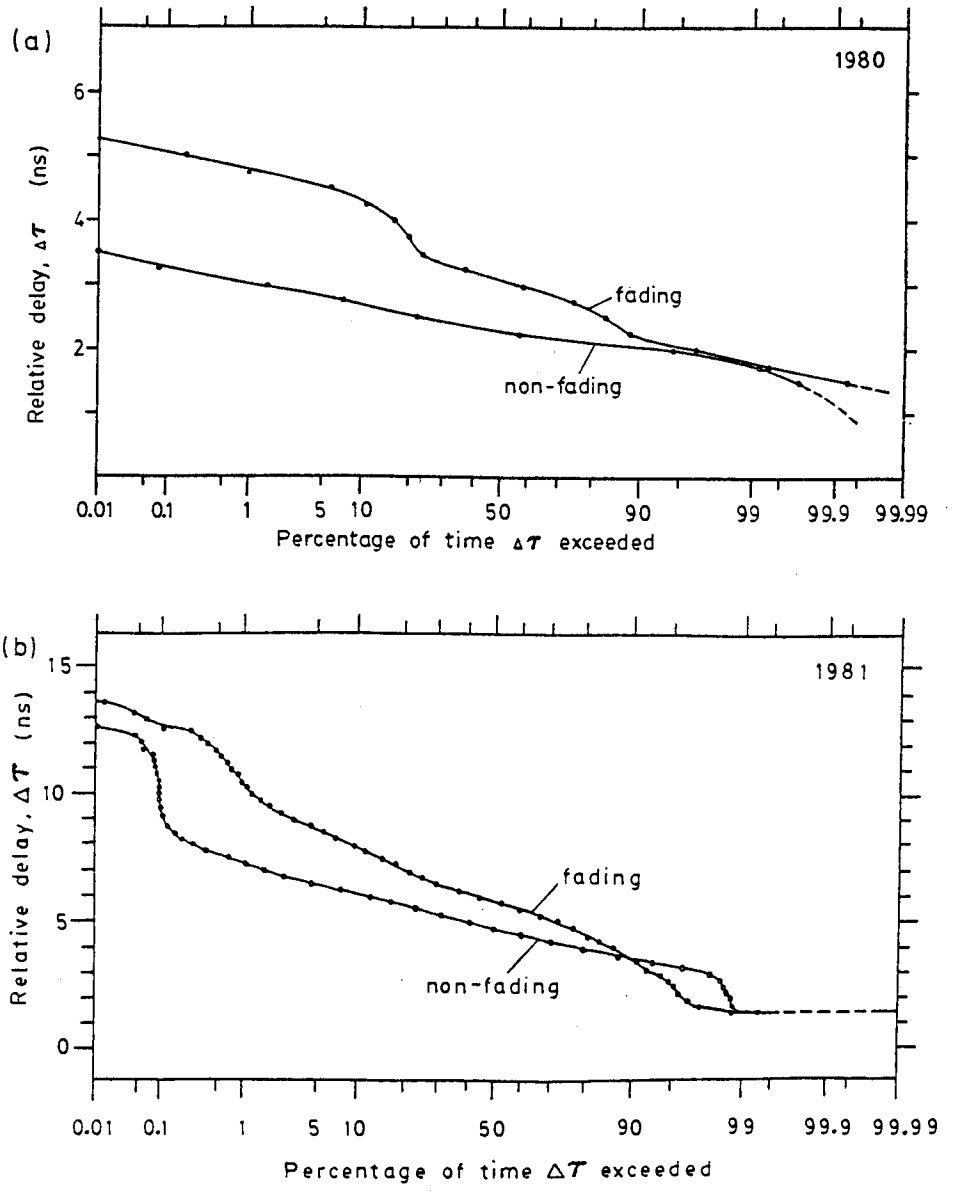

Fig. I.3.9 Distributions of the delay time of the second ray relative to the main ray during the 1980 and 1981 experiments, plotted using Normal Probability Coordinates.

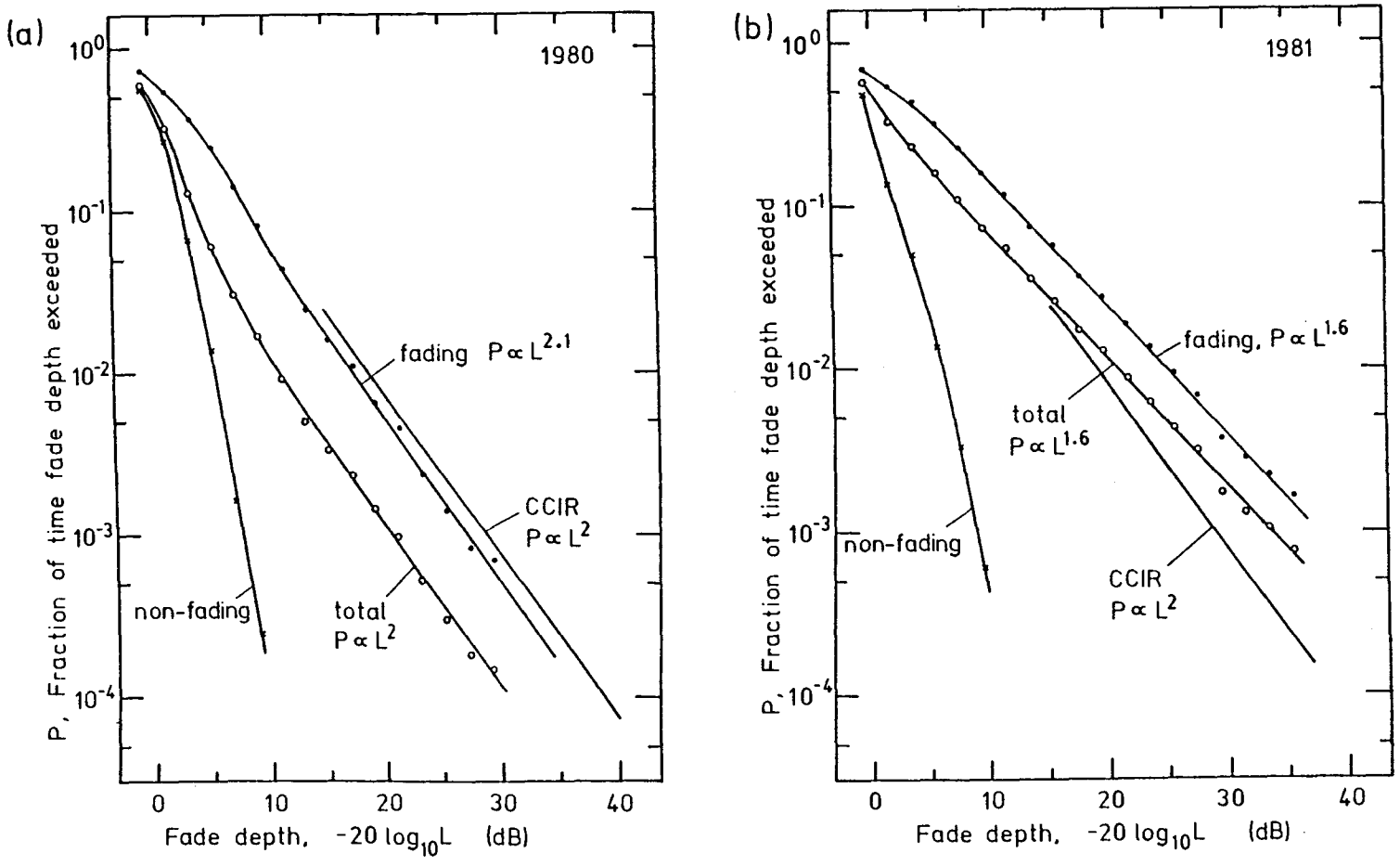

Fig. I.4.1 Distributions of the signal fade depth observed in the 1980 and 1981 experiments.

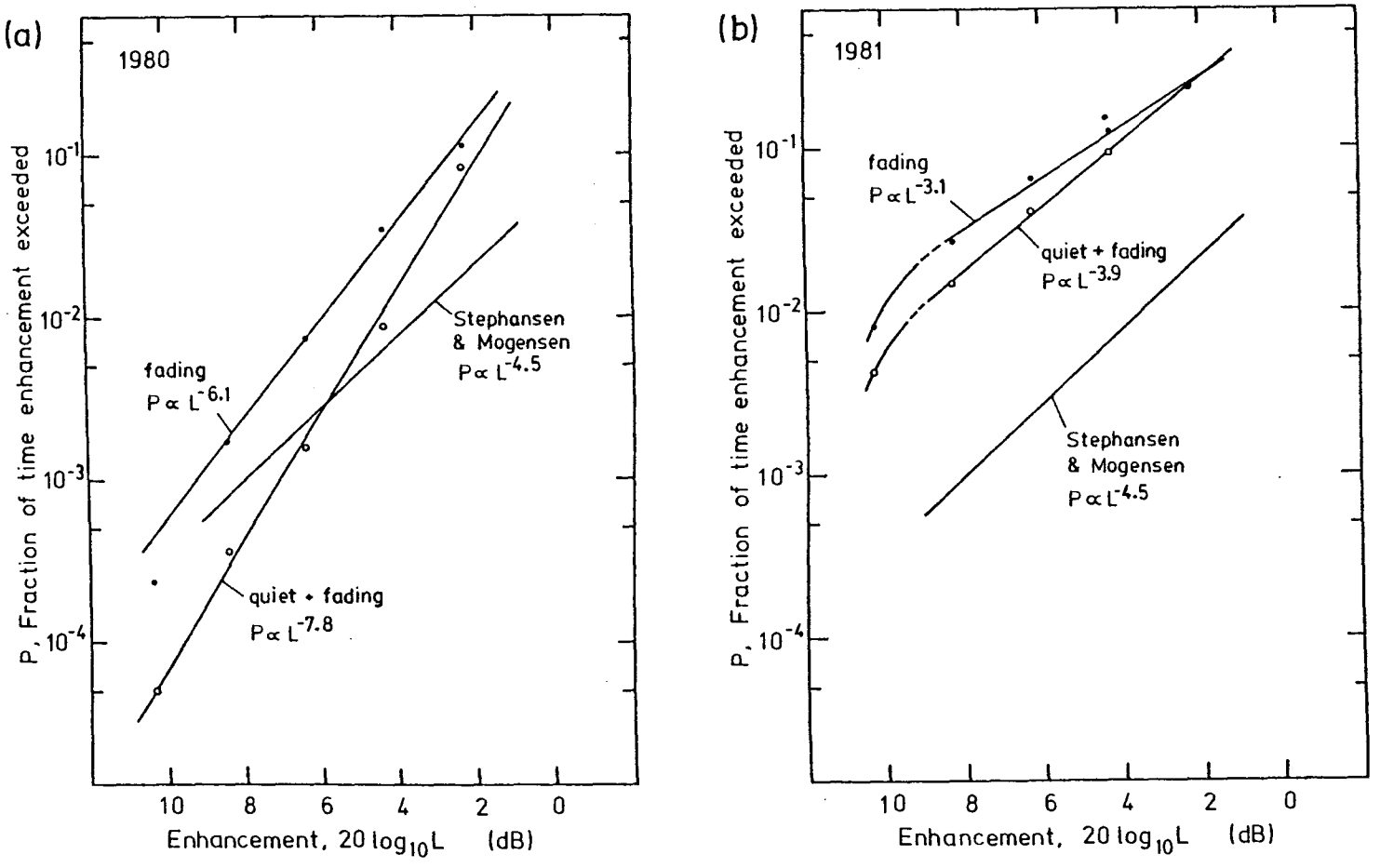

Fig. I.4.2 Distributions of the signal enhancement observed in the 1980 and 1981 experiments.

REFERENCES

[1] Webster, A.R. and W.I. Lam, "Operation of an experimental microwave link between Otter Lake, NB and Aylesford, NS". Final report, DSS Contract no. 18ST.36001-0-3173. CRC, Ottawa, Canada, 1981.

[2] Lam, W.I. and A.R. Webster, "A study of measurement and analysis of microwave propagation conditions across the Bay of Fundy". Final report, DSS Contract no. 03SU.36001-1-1054. CRC, Ottawa, Canada, July 1982.

[3] Webster, A.R. and W.I. Lam, "Microwave propagation across the Bay of Fundy. I - main path angle-of-arrival". Proc. of Third International Confr. on Antennas and Propag. (Icap-83), pp. 2.286-2.289. IEE and URSI, England. Apr 1983.

[4] Lam, W.I. and A.R. Webster, "Microwave propagation across the Bay of Fundy. II - multipath angles-of-arrival and delays". Proc. of Third International Confr. on Antennas and Propag. (ICAP-83), pp. 2.290-2.293. IEE and URSI, England. Apr 1983.

[5] Webster, A.R. and W.I. Lam, "Microwave multipath from sea reflections - the Bay of Fundy". Proc. URSI Commission F 1983 Symposium, Lovuvain-la-Neuve, Belgium. ESA SP-194, pp. 25-30. June 1983.

[6] Norton, K.A., L.E. Vogler, W.V. Mansfield, and P.J. Short, "The probability distribution of the amplitude of a Constant vector plus a Rayleigh-distributed vector". Proc. I.R.E., vol. 43, pp. 1354-1361, Oct 1955.

[7] Lam, W.I., The Propagation of Microwaves on Line-of-Sight Oversea Paths. Ph.D. Thesis. The Univ. of Western Ontario, London, Canada, Apr 1983.

[8] Segal, B. and R.E. Barrington, "Tropospheric refractivity atlas for Canada". CRC Report no. 1315-E, Ottawa, Dec 1977.

[9] International Radio Consultative Committee (CCIR), "Propagation data required for line-of-sight radio-relay systems". XV-th Plenary Assemble, Report 338-3 (mod. F), Geneva, 1982.

[10] Stephansen, E.T. and G.E. Mogensen, "Experimental investigation of some effects of multipath propagation on a line-of-sight path at 14 GHz". IEEE Trans. Comm., vol. COM-27(3), pp. 643-647, Mar 1979.

Part II

A VERY WIDE APERTURE ARRAY AS AN ALTERNATIVE DIAGNOSTIC SYSTEM -- SOME PRELIMINARY TESTS

II.1 INTRODUCTION

The diagnostic system used in gathering the microwave propagation results presented in Part I of this report, was developed to measure angles-of-arrival, amplitude and relative delay times of separate rays in a multipath situation. Additionally, the behaviour of the direct ray under single path conditions can be monitored on a routine basis. Much valuable data has been accumulated and presented in this and previous reports, and it is anticipated that more information will be extracted.

While these data are quite comprehensive and the results extremely useful, two aspects of the overall scheme present some difficulties in practice. First, the wide-band stepped frequency arrangement, together with the general complexity of the system, necessitates the presence of high calibre personnel during the operation of the system; this reduces its effectiveness from the point of view of portability and of long term measurements. Second, the extraction of the parameters associated with the individual paths under extreme conditions, while straightforward in principle, has proved to be tedious and

very time-consuming in practice. For these reasons, it is proposed that the possibility of developing a much simpler system be investigated, that is, simpler from the point of view of both operation and subsequent analysis. To do this, it seems clear that some of the comprehensiveness of that data from the original diagnostic system must be sacrificed. However, a wide aperture array operating at a single frequency will provide information on the number of paths together with an estimate of the amplitude and angle-of-arrival of each path, information which would provide considerable insight into the basic propagation characteristics, at the expense of delay times between paths.

II.2 THE BASIC PRINCIPLE

Since perturbations from the normal are expected to take place in the vertical plane, the basic idea is to sample the wave amplitude and phase across a very wide vertical aperture with the object of separating the contributions from different rays in a multipath situation. If estimates of the complex amplitude across the aperture are available, then a Fourier Transform of these estimates immediately transforms into the angle-of-arrival domain (see final report D.S.S. Contract 19ST.36001-2-0454).

Suitable weighting may be included at this stage and, in fact, once accurate complex amplitude estimates are recorded, the data may be manipulated at will. The total aperture width (L_λ) determines the resolution in angle ($\sim 1/L_\lambda$ radians), while the degree of filling of the aperture determines the unambiguous angular range ($\sim 1/d_\lambda$ rads where d_λ is the element separation in wavelengths). A 12-element array with elements spaced by 57 wavelengths, for example, provides a resolution of about 0.1 deg in a range of 1 deg; these numbers represent typical desired values.

II.3 PRELIMINARY CONSIDERATIONS

The object of the work described here is to investigate some practical aspects of the implementation of such a wide-aperture system. Central to the whole scheme is the need to measure accurately the complex amplitude at each element under severe fading conditions. To do this, not only is an accurate estimate of the amplitude required, but also the phase measurements should not be sensitive to environmental changes. From experience gained in operating the original diagnostic system, this suggests a minimum of 40 dB S/N ratio under normal conditions and the use of identical elements with mixers mounted immediately behind

the receiving antennas. Operational simplicity is also a major consideration. Some of these aspects are addressed below.

II.3.1 REQUIRED SIGNAL LEVELS

A basic system layout is shown in Fig. II.1 assuming a path length of 50 km, an operating frequency of 16.5 GHz and a transmitted power of 20 dBm. The rather high frequency ($\lambda \sim$ 1.8 cm) is suggested in order to keep the physical size of the array within reasonable bounds ($\sim 700\ \lambda$, i.e. 12.5 m). Bandwidths of 10 KHz and 30 KHz are assigned to the array channel and reference channel respectively. The appropriate use of 20 dB horns and standard 37 dB (2-ft diameter) dishes is recommended; a mixer loss of 8 dB is assumed (see II.3.3). As a result of this, S/N ratios of 46 dB and 58 dB for signal and reference channels are expected.

II.3.2 FREQUENCY STABILITY

In order to maintain the reference channel even under extreme fading conditions, a phase-locking approach is suggested. In its simplest form, this requires a channel bandwidth sufficient to accommodate drifts in the first intermediate frequency. Two oscillators manufactured by Frequency West Inc and operating at 16.530 and 16.650 GHz were fed to a standard diode mixer (Aertech) to produce a nominal intermediate frequency of 120 MHz. Sheltered from

rain, but otherwise open to the environment, this arrangement was operated for several weeks over a temperature range of 18°C or so and the intermediate frequency monitored. The maximum range in frequency at 120 MHz was found to be 9.5 KHz with a 98 % range of about 7 KHz. The oscillators are internally temperature controlled and no dependence on ambient temperature was observed. In view of this, a standard crystal 30 KHz bandwidth IF amplifier is recommended for the reference channel to guarantee the main phase lock, with standard 10 KHz bandwidth for the signal channel.

II.3.3 MIXER PERFORMANCE

Tests were performed in the outside environment to determine the phase stability of typical mixers. The basic arrangement involved the reception of signals on two horn antennas, spaced 1 m apart, over a short transmission path. The phase of the two signals derived from two mixers (Aertech MX18000A) fed by equal local oscillator waveguide sections was compared over several weeks and under varying conditions (sun, rain, snow, temperature 0-20°C). The maximum variation in phase observed was ±8°. Part of this variation might be due to changes in unavoidable reflections over the short path, but in any event this value represents the maximum expected in a full system.

Tests were performed on an alternate mixer (Magnum MM94) which is obtainable in flat-pack form suitable for

waveguide installation and is reasonably priced (US $250.). Direct measurements indicate the following:

Conversion loss	R.F.-I.F.	8.2 dB
Isolation	R.F.-I.F.	28 dB
	L.O.-I.F.	> 30 dB
	L.O.-R.F.	> 30 dB
Minimum L.O. power (< 1 dB down)		0 dBm

Subject to acceptable phase performance, this mixer appears to be very suitable for the application envisaged.

II.3.4 HORN ANTENNAS

Simple identical horn antennas with gain 20 dB are suggested for the array elements. Partly due to availability and cost considerations for commercial horns, three such antennas were designed and built in-house following standard design procedures for optimum pyramidal horns. The various properties shown in Fig. II.2 were measured and the performance appears to be quite satisfactory, although the slight discrepancy between theoretical and measured gain will be noted.

II.3.5 ANTENNA SWITCHING

In order to minimize phase shifts of equipment origin, it is desirable to use a single main signal receiver and to switch between array elements. In order to obtain a rapid sweep across the aperture (say, a maximum of 10 ms per element) an electronic switching arrangement is desirable.

A typical arrangement for a 16-element array is shown in Fig. II.3 together with details of a single switch using MPN 3401 diodes. From the diode specifications, such a diode arranged in series with a 50 Ω line should provide ON/OFF attenuations of 0.1/30 dB; direct measurements give attenuations of 0.4/27 dB. Better isolation is required when the switch is off and an extra 20 dB is provided by the inclusion of shunt diodes as in Fig. II.3. With the switching arrangement shown, only the switches immediately at the antennas plus the final switch need to be shunt/series to guarantee sufficient isolation (> 45 dB); the remainder may be the simpler series-only. Further tests need to be conducted to check the phase stability of the total switching system.

II.4 CONCLUSIONS

From the tests described here, it seems that the development of a full wide-aperture system is feasible. Additional tests on waveguide properties (custom built T-junctions, waveguide-coxial transitions, tuning slugs etc.) have been performed which indicate that the custom-building of the hardware is also feasible given the facilities available.

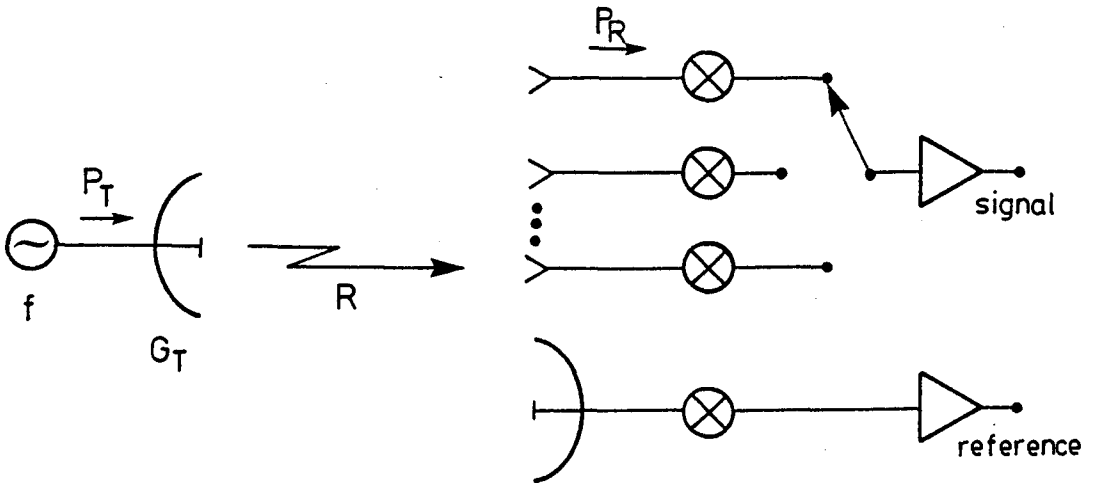

f = 16.5 GHz
λ = 0.0182 m.
R = 50 km
P_T = 20 dBm
G_T = 37 dB
G_R = 20 dB sig.
= 37 dB ref.
δf = 10 kHz sig.
= 30 kHz ref.
G_M = -8 dB
G_P = 20 dB
T_A = 100° K
T_M = 2000° K
T_P = 850° K

<u>With Mixer Input as Reference Point</u>

Signal: $P_R|_{dBm} = -131 + G_T|_{dB} + G_R|_{dB}$

⟶ -74 dBm signal
-57 dBm reference

Noise: System Temperature ~7550° K

⟶ -120 dBm signal
-115 dBm reference

<u>Signal: Noise Ratio</u>
Signal channel ⟶ 46 dB
Reference channel ⟶ 58 dB

Fig. II.1 System layout and received s:n ratio.

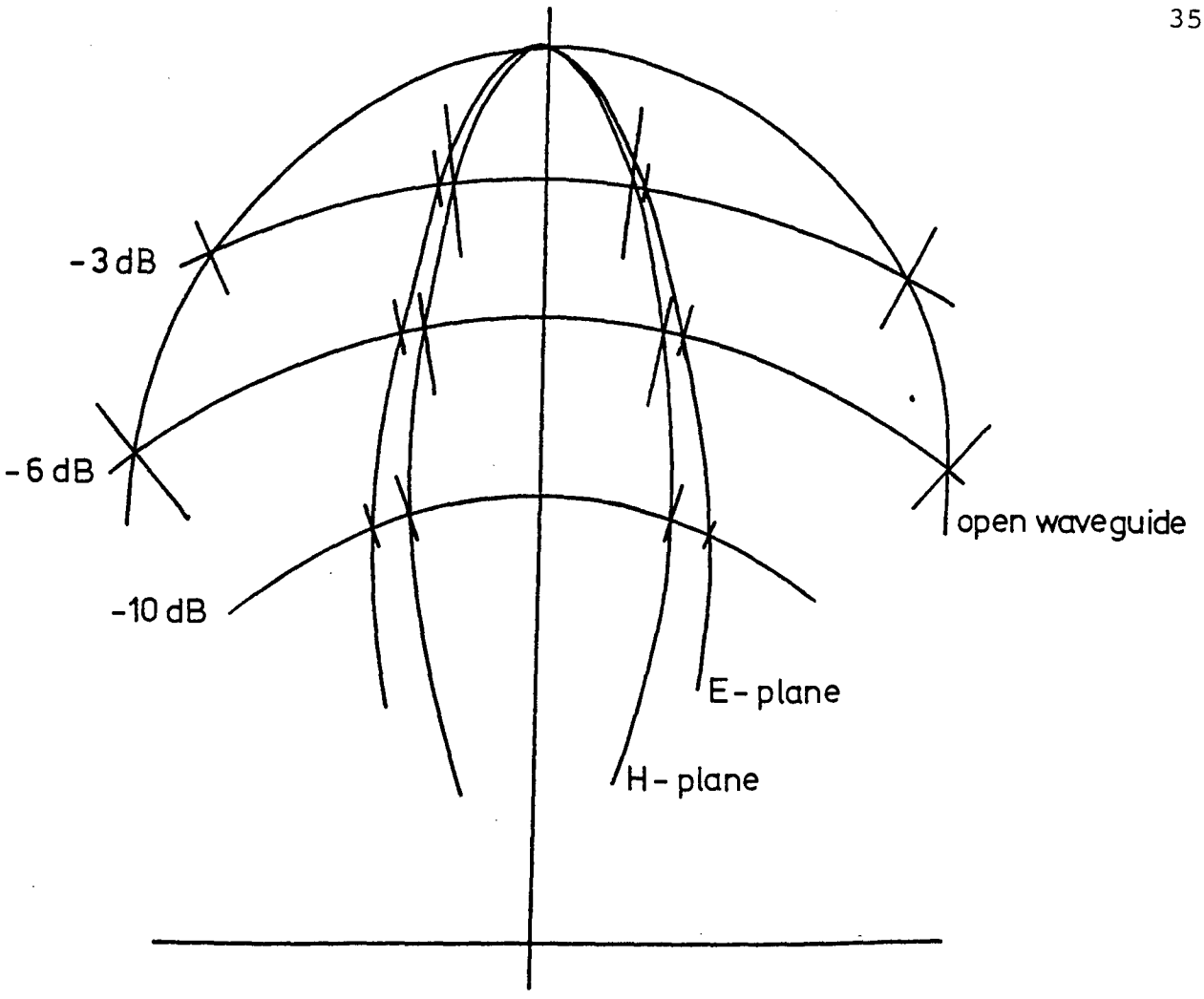

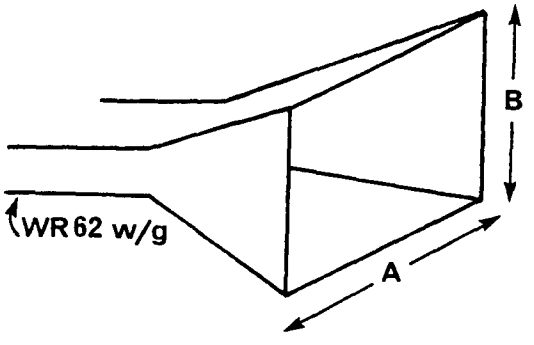

Measured Values (16.5 GHz)

Dimensions: A = 8.217cm, B = 6.402cm.

Beamwidth (3dB): H - plane ± 6.5°

E - plane ± 7.5°

Horn gain over open wave guide:	13.0 dB
Open w/g over isotropic :	5.8dB
Horn gain over isotropic :	18.8dB

Voltage S.W.R. < 1.1

Fig. II.2 20dB optimum pyramidal horn characteristics

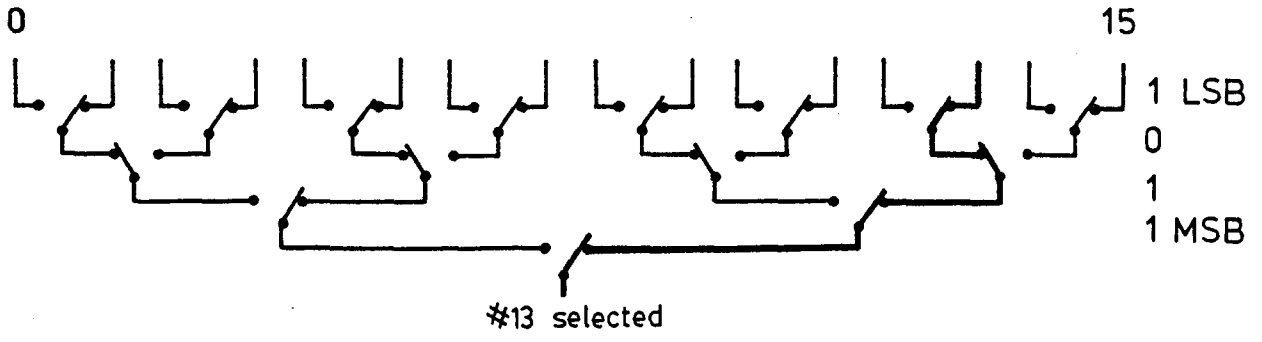

Typical switch (50Ω lines)

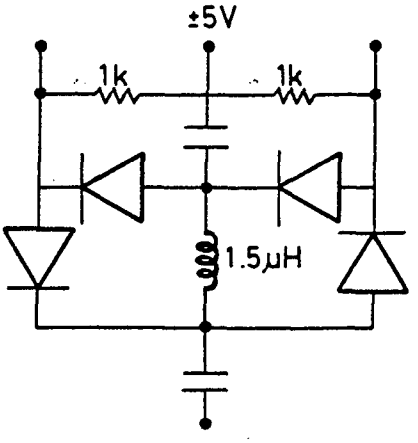

MPN 3401 diodes

forward resistance ~ 0.5Ω @4mA

reverse capacitance ~0.8pF~ j1650Ω @ 120MHz

Fig. II.3 Typical antenna switching system

ACKNOWLEDGEMENTS

The close cooperation of Maritime Telegraph and Telephone Company and New Brunswick Telephone Company during the experiments is very much appreciated. The authors would like to acknowledge the useful discussions with personnel at CRC and in the Centre for Radio Science.

The authors would also like to thank Mr. M.P. Pothier for efforts beyond his normal duties at M.T.& T., Mrs. M. Meighen for help in the typing, and Ms. S. Frank for help in drawing some of the diagrams.